Research Article

CdSe Quantum Dot-Sensitized Au/TiO₂ Hybrid Mesoporous Films and Their Enhanced Photoelectrochemical Performance

Liping Liu[1,2], Gongming Wang[2], Yat Li[2], Yadong Li[1] (✉), and Jin Z. Zhang[2] (✉)

[1] Department of Chemistry, Tsinghua University, Beijing 100084, China
[2] Department of Chemistry and Biochemistry, University of California, Santa Cruz, CA 95064, USA

ABSTRACT

Novel CdSe quantum dot (QD)-sensitized Au/TiO₂ hybrid mesoporous films have been designed, fabricated, and evaluated for photoelectrochemical (PEC) applications. The Au/TiO₂ hybrid structures were made by assembly of Au and TiO₂ nanoparticles (NPs). A chemical bath deposition method was applied to deposit CdSe QDs on TiO₂ NP films with and without Au NPs embedded. We observed significant enhancements in photocurrent for the film with Au NPs, in the entire spectral region we studied (350–600 nm). Incident-photon-to-current efficiency (IPCE) data revealed an average enhancement of 50%, and the enhancement was more significant at short wavelength. This substantially improved PEC performance is tentatively attributed to the increased light absorption of CdSe QDs due to light scattering by Au NPs. Interestingly, without QD sensitization, the Au NPs quenched the photocurrent of TiO₂ films, due to the dominance of electron trapping over light scattering by Au NPs. The results suggest that metal NPs are potentially useful for improving the photoresponse in PEC cells and possibly in other devices such as solar cells based on QD-sensitized metal oxide nanostructured films. This work demonstrates that metal NPs can serve as light scattering centers, besides functioning as photo-sensitizers and electron traps. The function of metal NPs in a particular nanocomposite film is strongly dependent on their structure and morphology.

KEYWORDS

1. Introduction

Solar hydrogen generation from water splitting using photoelectrochemical (PEC) cells and photovoltaic (PV) cells has attracted much attention in the past decade, as it is one of the most promising approaches for energy production [1–3]. Since the initial report of photocatalytic splitting of water on TiO₂ electrodes in 1972 [1], much effort has been made to improve the solar-to-hydrogen efficiency of PEC cells [4–7]. Semiconductor metal oxides, such as TiO₂, ZnO, and WO₃, with various film morphologies have been investigated for PEC water splitting [8–12].

Despite the fact that these metal oxides are inexpensive and chemically stable, most of them have large bandgaps and thus, limited visible light absorption. In order to enhance their visible light absorption for solar energy conversion, various approaches have

---

been taken, including dye and quantum dot (QD) sensitization as well as elemental doping. For instance, transition metals as well as nitrogen and carbon have been used as dopants to reduce their bandgap energy for enhancing visible light absorption [10, 13–17]. Alternatively, organic dyes and inorganic QDs have been utilized as visible light absorbers to sensitize the metal oxides [18, 19].

It has been reported that metal nanoparticles (NPs), such as Au and Ag, can enhance the photoresponse of semiconductors. For example, Au and Ag NPs deposited on polycrystalline Si thin films have been found to significantly increase the light absorption of the Si film and raise solar the electricity conversion efficiency of the Si solar cells [20, 21]. It was suggested that the metal NPs can act as a light trapping agent inside the Si film. Similar enhancement of PEC performance has been reported for nanostructured semiconductor–metal composite films [22–25], although the mechanism responsible for the observed enhancement is not yet fully understood. Tatsuma et al. suggested that the Au or Ag NPs serve as light sensitizers, similar to organic dyes, since the photoresponse of these TiO_2–metal composite films is consistent with the absorption spectra of Au or Ag NPs [25, 26]. Chen et al. also observed similar enhancement in photocurrent in ZnO nanowires incorporating Au NPs [18]. It was believed that the Au NPs act as photosensitizers and photogenerated electrons can be transferred from Au NPs to the connected ZnO nanowires by the force of the Schottky Au–ZnO contact. However, no incident-photon-to-current efficiency (IPCE) data were presented to directly confirm the photoactivity of the Au/ZnO composite film in the visible region. Very recently, Nishijima et al. reported plasmon-assisted photocurrent generation from a Au nanorods/TiO_2 electrode using visible to near infrared light [27]. In this case, the Au nanorods are elaborately arrayed on the surface of a TiO_2 single crystal.

Alternatively, Kamat et al. have proposed that another role of noble metal NPs in semiconductor–metal composite films, e.g., Au/TiO_2 NPs, is to help separate the photogenerated charges and, thus, improve the interfacial charge transfer kinetics [24, 28, 29]. The noble metal NPs act as electron sinks or traps to accumulate the photogenerated electrons, which can minimize charge recombination in the semiconductor films. A 40% improvement in hole transfer efficiency from the semiconductor film to the electrolyte was observed [28]. The IPCE data showed that there is no photoresponse in the absorption region of Au NPs. In this case, the Au NPs did not act as a light sensitizer, and increasing amount of Au NPs led to a gradual decrease of the photocurrent in the PEC cells [18, 29].

Besides acting as photosensitizers for charge injection or as electron traps for facilitating charge separation, noble metal NPs can also act as the light trapping or scattering agent in semiconductor–metal structures [20, 30–33]. Ag and Au NPs have strong absorption in the visible region due to surface plasmon resonance (SPR) absorption as a consequence of collective electron oscillation in response to electromagnetic field radiation [34]. Metal NPs can exhibit significant Rayleigh scattering, especially when their size is comparable to, or larger than, the wavelength of light. While the scattering can occur at any wavelength for a given sized particle, one may expect enhanced scattering as well as absorption, in the SPR region.

Here we report, for the first time, a synergistic effect observed in CdSe QD-sensitized Au/TiO_2 hybrid structures. Figure 1 shows a schematic diagram of this three-component nanocomposite structure. In the Au/TiO_2 hybrid structure, the Au NPs were embedded into TiO_2 nanoparticle clusters by assembling them together [35, 36], which ensured that the Au NPs have good contact with the TiO_2 NPs, and the CdSe QDs were deposited on the Au/TiO_2 films through a chemical bath deposition (CBD) process [37]. This synergistic enhancement is proportional to the amount of Au NPs embedded in the range of 0–5 wt.%, which cannot be simply explained by the Au NPs acting as photosensitizers or electron traps. Instead, we tentatively suggest that the synergistic enhancement is due to increased light absorption of the CdSe QDs as sensitizers for TiO_2, resulting from enhanced light scattering caused by Au NPs. This explanation is consistent with all of our experimental observations. The specific function of the metal NPs is believed to depend strongly on the structural or morphological details of the nanocomposite films and devices.
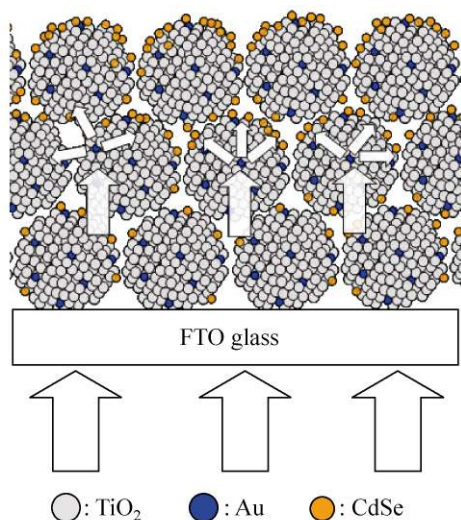
Figure 1 Schematic illustration of a CdSe QD-sensitized Au/TiO₂ film. When the film is irradiated by light, enhanced scattering by Au NPs is suggested to increase the effective light absorption of the CdSe QDs as sensitizers for TiO₂, and thereby the overall photoresponse of the nanocomposite film

2. Experimental

2.1 Synthesis of TiO₂ nanoparticles, Au nanoparticles and Au/TiO₂ hybrid mesoporous spheres

TiO₂ and Au NPs were synthesized followed the procedure reported in our previous work [38, 39]. To synthesize the TiO₂ NPs, NH₄HCO₃ (1 g), cyclohexane (5 mL), oleic acid (15 mL), and triethylamine (5 mL) were mixed together at room temperature with stirring, followed by addition of 1 mL of titanium tetraisopropoxide (Ti(OPr)₄) dropwise into the solution and stirring for 2 min. The solution was then transferred to an autoclave at 150 °C for 24 h. The TiO₂ NPs deposited at the bottom of the autoclave could be re-dissolved in cyclohexane. For the synthesis of Au NPs, 2 mL of oleylamine that contained 20 mg HAuCl₄ was dissolved in 20 mL of hexane. The solution was then transferred to an autoclave and put in an oven at the temperature of 70 °C for 8 h. After the reaction, the Au NPs were precipitated from the reaction solution by adding ethanol, and then re-dissolved in cyclohexane.

The synthesis of the Au/TiO₂ hybrid colloidal spheres utilized an emulsion-based bottom-up self-assembly (EBS) method [35, 39]. A mixture of 5 mL of TiO₂ NP solution (10 mg/mL) and 0.5 mL of Au NP solution (2 mg/mL) was added to 40 mL of an aqueous solution containing sodium dodecyl sulfate (SDS) surfactant (0.2 g). The mixture was emulsified by ultrasonic treatment together with strong stirring. The cyclohexane was evaporated by heating at about 70 °C with constant stirring for 3 h to assemble the NPs into colloidal spheres, which were then separated from the aqueous solution by centrifugation.

2.2 Fabrication of CdSe QD-sensitized Au/TiO₂ nanocomposite films

100 mg of Au/TiO₂ colloidal spheres were dissolved in 1 mL of water, and mixed with 80 mg of poly(ethylene glycol) (PEG, M_w = 3350) to form a viscous solution. A film was made by spin-coating 100 μL of Au/TiO₂ sol–gel NP solution at 500 r/min for 1 min on fluorine-doped tin oxide (FTO) glass, followed by drying at 100 °C for 30 min and calcining at 550 °C for 1 h in air. Pristine TiO₂ mesoporous films were made using the same EBS method under similar conditions. CdSe QDs were deposited on the Au/TiO₂ film and TiO₂ film using a CBD method. Cadmium acetate Cd(Ac)₂ was used as Cd source and sodium selenosulfate (Na₂SeSO₃) was the Se source. The Na₂SeSO₃ aqueous solution was prepared by refluxing Se powder in Na₂SO₃ solution for 24 h. 10 mL of a solution containing 0.1 mol/L Cd(Ac)₂ and 0.25 mol/L sodium citrate was mixed with 10 mL of 0.15 mol/L Na₂SeSO₃ solution. Then, the films were vertically immersed into this solution at 50 °C for 20 min, and then washed with water to remove the loosely attached CdSe QDs. The above process was then repeated in another cycle in order to increase the loading of CdSe QDs. Finally, the films were allowed to dry in air.

2.3 Characterization

Ultraviolet-visible (UV–Vis) absorption spectra were measured using a Hewlett–Packard 8452A diode array spectrophotometer. Powder X-ray diffraction (PXRD) analysis was conducted on a MINIFLEX diffractometer operating at 30 kV/15 mA using Cu *K*α radiation. A JEOL model JEM-1200EX transmission electron microscope (TEM) was used for the low-resolution TEM studies.

PEC studies (linear sweep voltammetry and IPCE)

were carried out on a Solartron 1280B (Oakridge, TN) with CorrWare 2, CorrView 2 and ZView 2 software. An Ag/AgCl (+0.198 V versus a standard hydrogen electrode) and Pt wire coil were used as the reference and counter electrodes, respectively. A 1000 W Xe lamp was utilized as a white-light source. The electrolyte used was a mixture of 0.2 mol/L Na_2S and 0.3 mol/L Na_2SO_3 aqueous solution, where Na_2S in solution acts as a hole scavenger and is oxidized into S_2^{2-} to prevent the photocorrosion of CdSe. Linear sweep voltammograms were measured at a scan rate of 10 mV/s at applied potentials from –0.6 V to 0.5 V in the dark and 100 mW/cm² illumination (AM 1.5). IPCE action spectra were measured at various wavelengths from 350 nm to 600 nm at an applied potential of 0.1 V (vs. Ag/AgCl).

3. Results and discussion

TEM images show that the as-prepared TiO_2 and Au NPs have uniform shape with an average diameter of 9 nm and 6 nm, respectively (Figs. 2(a) and 2(b)). Figure 2(c) shows the Au/TiO_2 hybrid colloidal spheres assembled from the TiO_2 and Au NPs using the EBS method. The average diameter of these colloidal spheres is about 50 nm. In the EBS process, the Au and TiO_2 NPs were thoroughly mixed and assembled into the spheres non-discriminately. Since the number of Au NPs was much less than that of TiO_2 NPs, it was expected that most of the Au NPs would be dispersed in the TiO_2 colloidal spheres as isolated units. The Au/TiO_2 films were calcined to ensure a good contact between Au and TiO_2 NPs. UV–Vis absorption spectra collected from TiO_2 NPs, Au NPs, and Au/TiO_2 colloid spheres are illustrated in Fig. 2(d). We observed an absorption peak of Au/TiO_2 colloid spheres centered at ~520 nm, which is consistent with the SPR absorption of Au NPs in solution.

During the synthesis of Au/TiO_2 colloidal spheres, organic oleic acid (OA) ligands were used to cap the constituent Au and TiO_2 NPs. To achieve strong interfacial interaction between all the NPs and avoid any adverse effects of OA capping ligands on PEC performance, we calcined the hybrid colloidal spheres in air to remove the ligands and generate mesoporous structures [36]. PXRD was used to characterize the
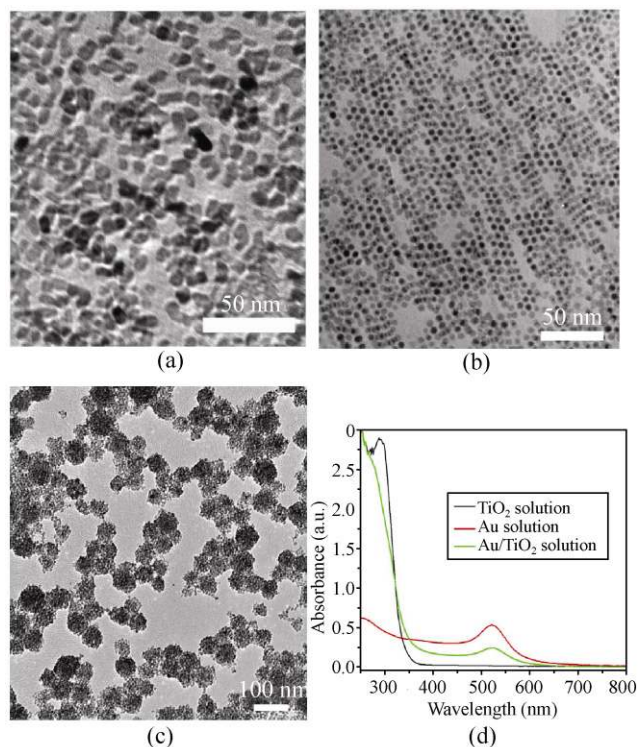

Figure 2 TEM images of (a) TiO_2 NPs, (b) Au NPs, and (c) Au/TiO_2 colloidal spheres. (d) UV–Vis spectra of TiO_2 NPs (solution), Au NPs (solution), and Au/TiO_2 colloidal spheres (solution)

calcined Au/TiO_2 films (Fig. 3). The dominant peaks can be indexed to the anatase TiO_2 pattern (JCPDS Card No: 21-1272). Although it is difficult to distinguish the Au (111) diffraction peak from the (004) peak of anatase TiO_2 due to peak broadening for the NPs, we clearly identified the secondary diffraction peaks of (200) and (220) crystal planes for Au in the PXRD pattern. The results confirmed the existence of Au NPs in the mesoporous structures, and that the Au NPs have a cubic structure. Moreover, no other impurity-related diffraction peaks were detected, indicating the sample has high purity.

Figure 4(a) shows the UV–Vis spectra of the TiO_2 and Au/TiO_2 films with different amounts of Au NPs. The pristine TiO_2 film was made from TiO_2 colloidal spheres as a control experiment. The apparent peaks near 320 nm are due to the FTO glass substrate as a background, that resulted in unreliable measurements at wavelengths near to, and shorter than, 300 nm. In general, the absorption is expected to continue to increase towards shorter wavelength in the UV and
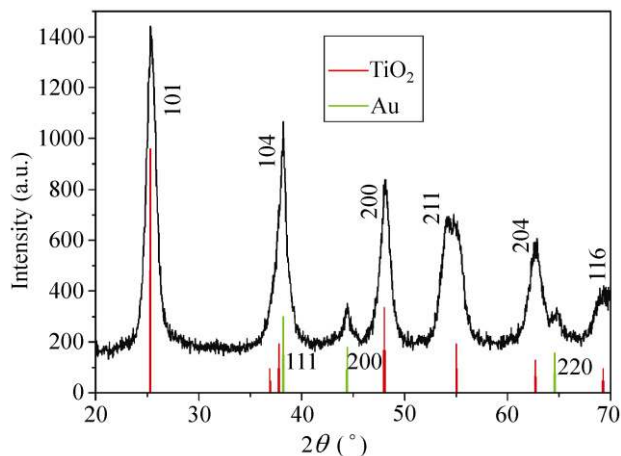
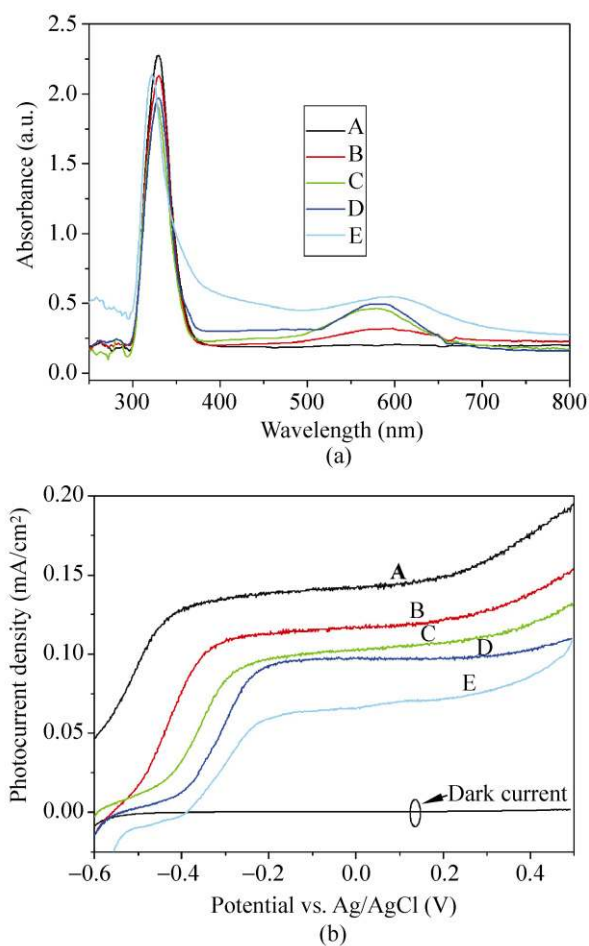**Figure 3** XRD pattern of Au/TiO$_2$ spheres after calcinations

Figure 4 (a) UV–Vis spectra (samples are solid) of pristine TiO$_2$ film (A) and Au/TiO$_2$ films with different amount of Au NPs: (B) 0.5 wt.%, (C) 1.5 wt.%, (D) 2.5 wt.%, (E) 5 wt.%. (b) Linear sweep voltammograms, collected at a scan rate of 10 mV/s at applied potential from –0.6 V to +0.5 V (vs. Ag/AgCl) from the corresponding TiO$_2$ film and Au/TiO$_2$ films in (a) in the dark and with light illumination of 100 mW/cm^2

near UV regions for most samples. For the pristine TiO$_2$ film sample, the absorption onset is around 360 nm, with minimal visible light absorption. In contrast, the Au/TiO$_2$ film showed strong absorption in the visible region due to the SPR of Au NPs, and the absorption increases with increasing Au NPs loading. In comparison to the Au/TiO$_2$ spheres in solution, the absorption peak of the Au/TiO$_2$ films was slightly red-shifted to about 580–590 nm after the calcination. The red-shift is likely due to the change in effective refractive index of the surrounding medium of Au NPs.

Photoelectrochemical properties of the fabricated nanocomposite films were studied by measuring the photocurrent as a function of applied potential. Figure 4(b) shows the linear sweep voltammograms recorded from TiO$_2$ and Au/TiO$_2$ films in the dark and with light illumination of 100 mW/cm^2 (A.M. 1.5). The Au/TiO$_2$ films have lower photocurrent than the pristine TiO$_2$ film, and the photocurrent decreased systematically with increasing loading of Au NPs. This reduction of photocurrent observed in Au/TiO$_2$ films is attributed to trapping of photogenerated electrons in TiO$_2$ by Au NPs, which is consistent with the observation reported previously by Kamat et al. [29].

To have a detailed characterization of the photo-response as a function of light wavelength, IPCE measurements were performed on these films. The IPCE was determined by the following equation

$$IPCE = (1240 \times I) / (\lambda \times J_{light}) \qquad (1)$$

where I is the photocurrent density, λ the incident light wavelength, and J_{light} is the measured irradiance. Figure 5 shows the IPCE results for both a TiO$_2$ film and a Au/TiO$_2$ film with 5 wt.% Au. The photoresponse of the TiO$_2$ film is minimal above 390 nm, and then increases dramatically when the photon energy is higher than the bandgap energy of TiO$_2$. The Au/TiO$_2$ film also showed minimal photoresponse above 390 nm, even though it absorbs visible light. The IPCE data clearly indicate that the Au NPs in this Au/TiO$_2$ hybrid structure are not functioning as photosensitizers for TiO$_2$. In fact, the incorporation of Au NPs reduced the IPCE of TiO$_2$. We believe that the lack of photoactivity in the visible region, e.g.,
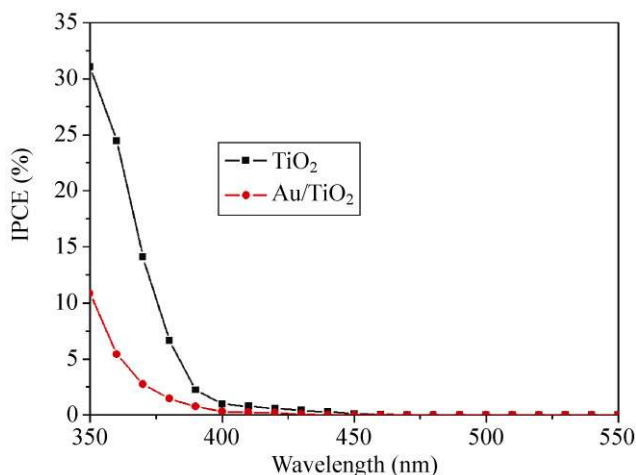
Figure 5 Measured IPCE spectra of TiO_2 film and Au/TiO_2 film (with 5 wt.% Au) in the region 350 nm to 550 nm at a potential of 0.1 V (vs. Ag/AgCl)

near the SPR region, is because photoexcited electrons in Au NPs are very short-lived and thereby unable to inject electrons into TiO_2 in an effective manner [40, 41]. The observed decrease in photocurrent in the near UV region is likely a result of trapping of photogenerated electrons in TiO_2 by Au NPs, as suggested previously in similar systems [24, 29, 42, 43]. In our case, the photosensitizing effect reported in previous studies is apparently weak in comparison to the trapping effect. The dominance of each effect may be critically dependent on the details of the nano-structure or morphology of the film. For instance, strong interaction between Au and TiO_2 NPs may favor the sensitizing effect since electron injection from Au NP to TiO_2 NP can then compete effectively with hot electron relaxation within Au NPs. In this study, the Au NPs are expected to be thoroughly mixed with TiO_2 NPs and embedded as isolated units in the metal oxide due to the low loading level, which is significantly different from previously reported Au/metal oxide nanocomposite structures. The function of Au NPs may be determined by the concentration of Au NPs and/or the coupling between the Au and TiO_2 NPs. This is an important issue that should be further investigated by using ultrafast dynamic studies to distinguish between the various competing kinetic processes.

Although the incorporation of Au NPs reduced both the photocurrent and IPCE for the Au/TiO_2 films

compared to pristine TiO_2 sample, we observed significantly enhanced photocurrent and IPCE for CdSe QD-sensitized Au/TiO_2 composite films compared to CdSe QD-sensitized TiO_2 films without Au NPs. Figure 6(a) shows the UV–Vis spectra of the CdSe QD-sensitized TiO_2 film and Au/TiO_2 films. Compared to the UV–Vis spectra of TiO_2 and Au/TiO_2 samples (Fig. 4(a)), the absorption of these sensitized films in the visible region was dominated by CdSe QDs, and therefore we did not observe an increase in Au SPR absorption with increasing Au NP
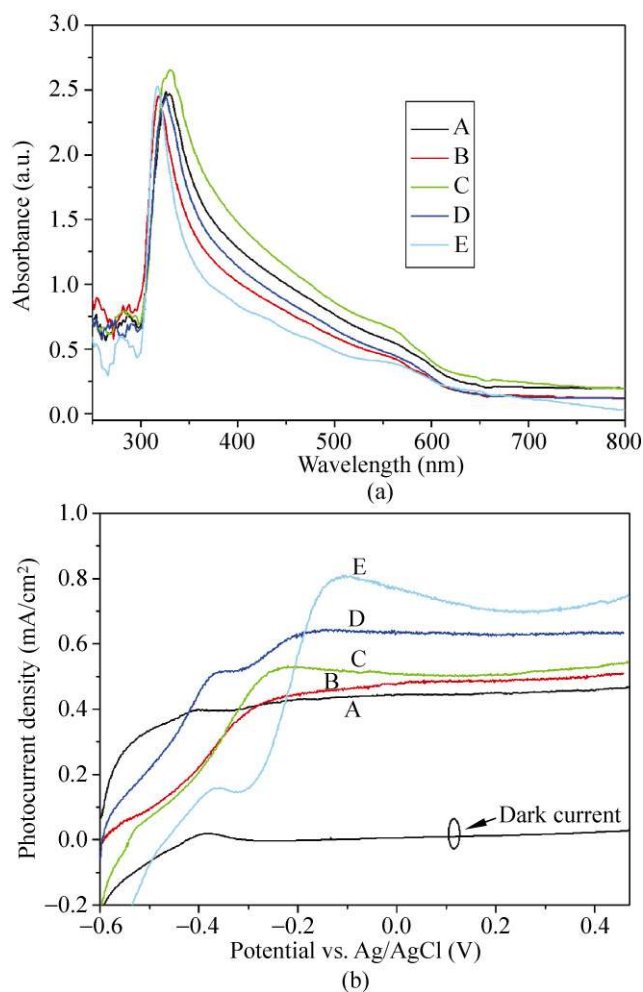

(a)

(b)

Figure 6 (a) UV–Vis spectra of CdSe QD sensitized-TiO_2 film (A) and CdSe sensitized Au/TiO_2 films with different amount of Au NPs: (B) 0.5 wt.%, (C) 1.5 wt.%, (D) 2.5 wt.%, (E) 5 wt.% (with blanking against FTO glass substrate as background, and the thickness of the films are almost the same). (b) Linear sweep voltammograms, collected at a scan rate of 10 mV/s at applied potential from –0.6 V to +0.5 V (vs. Ag/AgCl) from the corresponding CdSe QD-sensitized TiO_2 and Au/TiO_2 films in (a), in the dark and with light illumination of 100 mW/cm^2

loading. There was no correlation between the overall absorption intensity and Au loading. This could be due to the possible variations of film thickness or CdSe QD density from sample to sample. In any case, the variation in sample optical density (OD) does not seem to be directly related to the loading of Au NPs. However, this small variation in sample OD does not affect the key observation of enhanced photoresponse resulting from Au NPs incorporation, which will be discussed next. What is important for PEC is the photocurrent, and the OD can be affected by many factors and is less critical than photocurrent for PEC.

The PEC properties of all these CdSe QD-sensitized nanocomposite films were carefully examined. As shown in Fig. 6(b), the I–V characteristics revealed pronounced photoresponses for all these films under light illumination of 100 mW/cm². As expected, the photocurrent of the CdSe QD sensitized nanocomposite films increased substantially compared to the non-sensitized samples. Since the CdSe QDs were deposited on the surface of the TiO₂ or Au/TiO₂ films, the internal structure of the TiO₂ or Au/TiO₂ films should remain essentially unchanged after the QD sensitization. Thus, the enhanced photocurrent is mostly due to absorption of light by CdSe QDs. More importantly, the CdSe QD-sensitized Au/TiO₂ films showed higher photocurrent than the one without Au NPs, and the photocurrent increased with the increased loading of Au NPs. The results unambiguously demonstrate the existence of a synergistic effect between CdSe QD and Au NPs. Since we have shown that the Au NPs cannot work as effective photo- sensitizers, but rather as electron traps in the Au/TiO₂ films, the significantly enhanced photocurrent in CdSe QD-sensitized TiO₂ in the presence of Au NPs must be due to another reason. We suggest that the observed synergistic effect of Au NPs and CdSe QDs in enhancing photocurrent is a result of increased light absorption by CdSe QDs caused by increased light scattering by Au NPs. The strong scattering from Au NPs can effectively increase the optical path of the incident light in the absorber layer [31, 33], as shown in Fig. 1, and thus, increase the effective absorption of light by CdSe QDs. This explanation is strongly supported by IPCE data that will be discussed later.

We noticed that the onset potential varied somewhat with Au NP loading but there is no simple or clear trend that can be established with regard to increasing loading of Au NPs. The change in onset potential has been observed in similar metal–metal oxide composite systems and been attributed to Fermi level re-equilibration in the composite nanostructure [22, 24]. In the two-component Au/TiO₂ system (Fig. 4(b)), the onset potential seems to shift towards more positive potential with increasing loading of Au NPs, indicating that the Fermi level moves downwards in energy. In the three-component CdSe QD-Au/TiO₂ system, the lack of a simple trend could be attributed to the complications caused by competing factors or the influence of the CdSe QDs in addition to Au/TiO₂.

To better understand the fundamental mechanism behind the improved photocurrent in the CdSe QD-sensitized Au/TiO₂ nanocomposite films, IPCE was measured in the region of 350–600 nm. Figure 7 shows IPCE results for the CdSe QD-sensitized TiO₂ and Au/TiO₂ film with 5 wt.% of Au NPs. In comparison to non-sensitized samples, the CdSe QD-sensitized Au/TiO₂ film showed enhanced IPCE in the entire wavelength we studied (350–600 nm) as the incorporation of small bandgap CdSe QDs substantially improved visible light absorption. There is no obvious enhancement of IPCE in the SPR region of Au NPs (~520 nm), thus, indicating that the enhancement is not related to the SPR or electro-magnetic enhancement effect of Au NPs. The data reveal substantially enhanced IPCE for the CdSe QD-sensitized Au/TiO₂ film compared to the one without Au NPs, which is consistent with the higher maximum photocurrent observed with the CdSe QD-sensitized Au/TiO₂ film. The IPCE increased consistently and monotonically from the long wavelength towards short wavelength (e.g., the percentage increased from 30% at 600 nm to 80% at 350 nm). It is well known that the light scattering cross section for a given particle with a specific size, Au NPs in the present case, increases with decreasing wavelength. Therefore, this wavelength-dependent IPCE enhancement, i.e., increased IPCE enhancement with decreasing wavelength, strongly suggests that the observed IPCE enhancement be related to light scattering by Au NPs. As we have discussed in relation to Figs. 4 and 5,
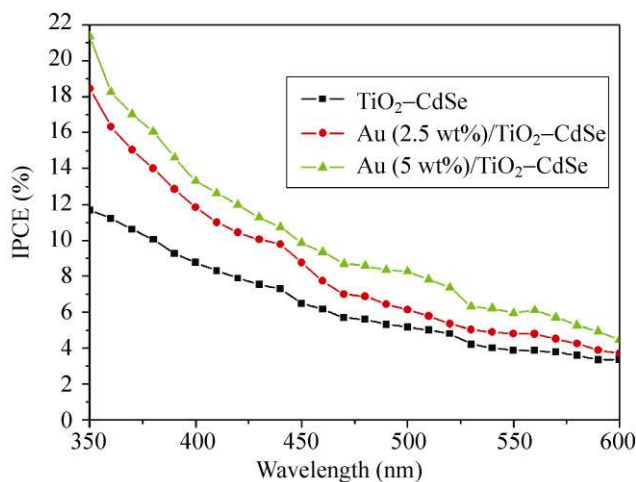
Figure 7 Measured IPCE spectra of CdSe QD-sensitized TiO$_2$ and Au/TiO$_2$ films (with 2.5 wt.% Au and 5 wt.% Au) in the region of 350 nm to 600 nm at a potential of 0.1 V (vs. Ag/AgCl)

the incorporation of Au NPs leads to a reduction in the photocurrent and IPCE of the pristine TiO$_2$ film due to the trapping or quenching of photogenerated electrons from TiO$_2$. Thus, the enhanced photocurrent and IPCE in CdSe QD-sensitized Au/TiO$_2$ composite films is most likely caused by increasing light absorption of CdSe QDs due to enhanced light scattering by Au NPs.

In principle, Au NPs can function as a photo-sensitizer to absorb visible light, or as impurity sites for electron trapping or light scattering. The dominance of a specific role played by the Au NPs is believed to strongly depend on the details of structure or morphology of the nanocomposite film. In this work, the Au NPs acted primarily as both electrons traps and light scattering centers. For Au/TiO$_2$ films without CdSe QD sensitization, the dominant role of Au NPs is to trap or quench photogenerated electrons in TiO$_2$ via UV and near UV light excitation. Light absorption and scattering of Au NPs in the visible region are relatively insignificant in contributing to the observed photocurrent. In contrast, for CdSe QD-sensitized Au/TiO$_2$ composite films, the photocurrent is do-minated by the visible light absorption of CdSe QDs. Therefore the incorporation of the Au NPs as light scattering centers became significant and enhanced the photocurrent of the composite film. In this case, electron trapping by Au NPs is relatively unimportant. The results suggest a promising approach for

improving the performance of metal oxide photo-electrodes in PEC cells and possibly PV device app-lications. Other metals, such as Ag, with SPR absorption may exhibit similar effects to Au, and further research is underway for comparative studies.

4. Conclusion

A novel CdSe QD-sensitized Au/TiO$_2$ nanocomposite has been designed, synthesized, and studied for PEC applications. Au NPs have been found to significantly enhance the photocurrent of CdSe QD-sensitized TiO$_2$ nanocomposite films. The enhancement is synergistic in that it is only occurs when both Au NPs and CdSe QDs are present at the same time. This effect is attributed to increased absorption of light by CdSe QDs as a result of increased light scattering due to Au NPs. This observation provides useful funda-mental insights for developing new nanostructures tailored for PEC cells and possibly other applications including PV cells.

Acknowledgements

References

[1] Fujishima, A.; Honda, K. Electrochemical photolysis of water at a semiconductor electrode. *Nature* **1972**, *238*, 37–38.

[2] Khaselev, O.; Turner, J. A. A monolithic photovoltaic-photoelectrochemical device for hydrogen production via

water splitting. *Science* **1998**, *280*, 425–427.

[3] Bak, T.; Nowotny, J.; Rekas, M.; Sorrell, C. C. Photo-electrochemical hydrogen generation from water using solar energy. Materials-related aspects. *Int. J. Hydrogen energy* **2002**, *27*, 991–1022.

[4] Heller, A. Hydrogen-evolving solar-cells. *Science* **1984**, *223*, 1141–1148.

[5] Hagfeldt, A.; Gratzel, M. Light-induced redox reactions in nanocrystalline systems. *Chem. Rev.* **1995**, *95*, 49–68.

[6] Murphy, A. B.; Barnes, P. R. F.; Randeniya, L. K.; Plumb, I. C.; Grey, I. E.; Horne, M. D.; Glasscock, J. A. Efficiency of solar water splitting using semiconductor electrodes. *Int. J. Hydrogen Energy* **2006**, *31*, 1999–2017.

[7] Rajeshwar, K. Hydrogen generation at irradiated oxide semiconductor-solution interfaces. *J. Appl. Electrochem.* **2007**, *37*, 765–787.

[8] Santato, C.; Odziemkowski, M.; Ulmann, M.; Augustynski, J. Crystallographically oriented mesoporous WO_3 films: Synthesis, characterization, and applications. *J. Am. Chem. Soc.* **2001**, *123*, 10639–10649.

[9] Wolcott, A.; Kuykendall, T. R.; Chen, W.; Chen, S. W.; Zhang, J. Z. Synthesis and characterization of ultrathin WO_3 nanodisks utilizing long-chain poly(ethylene glycol) *J. Phys. Chem. B* **2006**, *110*, 25288–25296.

[10] Park, J. H.; Kim, S.; Bard, A. J. Novel carbon-doped TiO_2 nanotube arrays with high aspect ratios for efficient solar water splitting. *Nano Lett.* **2006**, *6*, 24–28.

[11] Ahn, K. S.; Yan, Y. F.; Lee, S. H.; Deutsch, T.; Turner, J.; Tracy, C. E.; Perkins, C. L.; Al-Jassim, M. Photoelectrochemical properties of N-incorporated ZnO films deposited by reactive RF magnetron sputtering. *J. Electrochem. Soc.* **2007**, *154*, B956–B959.

[12] Wolcott, A.; Smith, W. A.; Kuykendall, T. R.; Zhao, Y. P.; Zhang, J. Z. Photoelectrochemical water splitting using dense and aligned TiO_2 nanorod arrays. *Small* **2009**, *5*, 104–111.

[13] Choi, W.; Termin, A.; Hoffmann, M. R. The role of metal ion dopants in quantum-sized TiO_2: Correlation between photoreactivity and charge carrier recombination dynamics. *J. Phys. Chem.* **1994**, *98*, 13669–13679.

[14] Asahi, R.; Morikawa, T.; Ohwaki, T.; Aoki, K.; Taga, Y. Visible-light hotocatalysis in nitrogen-doped titanium oxides. *Science* **2001**, *293*, 269–271.

[15] Torres, G. R.; Lindgren, T.; Lu, J.; Granqvist, C. G.; Lindquist, S. E. Photoelectrochemical study of nitrogen-doped titanium dioxide for water oxidation. *J. Phys. Chem. B* **2004**, *108*, 5995–6003.

[16] Qiu, X. F.; Zhao, Y. X.; Burda, C. Synthesis and characterization of nitrogen-doped group IVB visible-light-photoactive metal oxide nanoparticles. *Adv. Mater.* **2007**,

19, 3995–3999.

[17] Hensel, J.; Wang, G. M.; Li, Y.; Zhang, J. Z. Synergistic effect of CdSe quantum dot sensitization and nitrogen doping of TiO_2 nanostructures for photoelectrochemical solar hydrogen generation. *Nano Lett.* **2010**, *10*, 478–483.

[18] Chen, Z. H.; Tang, Y. B.; Liu, C. P.; Leung, Y. H.; Yuan, G. D.; Chen, L. M.; Wang, Y. Q.; Bello, I.; Zapien, J. A.; Zhang, W. J.; Lee, C. S.; Lee, S. T. Veertically aligned ZnO nanorod arrays sentisized with gold nanoparticles for Schottky barrier photovoltaic cells. *J. Phys. Chem. C* **2009**, *113*, 13433–13437.

[19] Tak, Y.; Hong, S. J.; Lee, J. S.; Yong, K. Fabrication of ZnO/CdS core/shell nanowire arrays for efficient solar energy conversion. *J. Mater. Chem.* **2009**, *19*, 5945–5951.

[20] Derkacs, D.; Lim, S. H.; Matheu, P.; Mar, W.; Yu, E. T. Improved performance of amorphous silicon solar cells via scattering form surface plasmon polaritons in nearby metallic nanoparticles. *Appl. Phys. Lett.* **2006**, *89*, 093103.

[21] Pillai, S.; Catchpole, K. R.; Trupke, T.; Green, M. A. Surface plasmon enhanced silicon solar cells. *J. Appl. Phys.* **2007**, *101*, 093105.

[22] Nakato, Y.; Shioji, M.; Tsubomura, H. Photoeffects on the potentials of thin metal films on a *n*-TiO_2 crystal wafer. The mechanism of semiconductor phtocatalsts. *Chem. Phys. Lett.* **1982**, *90*, 453–456.

[23] Zhao, G. L.; Kozuka, H.; Yoko, T. Photoelectrochemical properties of dye-sensitized TiO_2 films containing dispersed gold metal particles prepared by sol-gel method. *J. Ceramic Soc. Jan* **1996**, *104*, 164–168.

[24] Chandrasekharan, N.; Kamat, P. V. Improved the photoelectrochemical performance of nanostructured TiO_2 films by adsorption of gold nanoparticles. *J. Phys. Chem. B* **2000**, *104*, 10851–10857.

[25] Tian, Y.; Tatsuma, T. Mechanisms and applications of plasmon-induced charge separation at TiO_2 films loaded with gold nanopaticles. *J. Am. Chem. Soc.* **2005**, *127*, 7632–7637.

[26] Tian, Y.; Tatsuma, T. Plasmon-induced photoelectrochemistry at metal nanoparticles supported on nanoporous TiO_2. *Chem. Commun.* **2004**, 1810–1811.

[27] Nishijima, Y.; Ueno, K.; Yokota, Y.; Murakoshi, K.; Misawa, H. Plasmon-assisted photocurrent generation from visible to near-infrared wavelength using a Au-nanorods/TiO_2 electrode. *J. Phys. Chem. Lett.* **2010**, *1*, 2031–2036.

[28] Dawson, A.; Kamat, P. V. Semiconductor-metal nano-composites. Photoinduced fusion and photocatalysis of gold-capped TiO_2 (TiO_2/gold) nanoparticles. *J. Phys. Chem. B* **2001**, *105*, 960–966.

[29] Subramanian, V.; Wolf, E.; Kamat, P. V. Semiconductor-metal composite nanostructures. To what extent do metal

nanoparticles improve the photocatalytic activity of TiO$_2$ films. *J. Phys. Chem. B* **2001**, *105*, 11439–11446.

[30] Schaadt, D. M.; Feng, B.; Yu, E. T. Enhanced semiconductor optical absorption via surface plasmon excitation in metal nanoparticles. *Appl. Phys. Lett.* **2005**, *86*, 063106.

[31] Catchpoleand, K. R.; Polman, A. Design principles for particle plasmon enhanced solar cells. *Appl. Phys. Lett.* **2008**, *93*, 191113.

[32] Nakayama, K.; Tanabe, K.; Atwater, H. A. Plasmonic nanoparticle enhanced light absorption in GaAs solar cells. *Appl. Phys. Lett.* **2008**, *93*, 121904.

[33] Smith, W.; Mao, S.; Lu, G. H.; Catlett, A.; Chen, J. H.; Zhao, Y. P. The effect of Ag nanoparticle loading on the photocatalytic activity of TiO$_2$ nanorod arrays. *Chem. Phys. Lett.* **2010**, *485*, 171–175.

[34] Zhang, J. Z.; Noguez, C. Plasmonic optical properties and applications of metal nanostructures. *Plasmonics* **2008**, *3*, 127–150.

[35] Bai, F.; Wang, D. S.; Huo, Z. Y.; Chen, W.; Liu, L. P.; Liang, X.; Chen, C.; Wang, X.; Peng, Q.; Li, Y. D. A versatile bottom-up assembly approach to colloidal Spheres from nanocrytstals. *Angew. Chem. Int. Ed.* **2007**, *46*, 6650–6653.

[36] Liu, L. P.; Hensel, J.; Fitzmorris, R. C.; Li, Y. D.; Zhang, J. Z. Preparation and photoelectrochemical properties of CdSe/TiO$_2$ hybrid mesoporous structures. *J. Phys. Chem. Lett.* **2010**, *1*, 155–160.

[37] Lokhande, C. D.; Lee, E. H.; Jung, K. D.; Joo, O. S. Ammonia-free chemical bath method for deposition of microcrystalline cadmium selenide films. *Mater. Chem. Phys.* **2005**, *91*, 200–204.

[38] Li, X. L.; Peng, Q.; Yi, J. X.; Wang, X.; Li, Y. D. Near monodisperse TiO$_2$ nanoparticles and nanorods. *Chem. Eur. J.* **2006**, *12*, 2383–2391.

[39] Liu, J. F.; Chen, W.; Liu, X. W.; Zhou, K. B.; Li, Y. D. Au/LaVO$_4$ nanocomposite: Preparation, characterization, and catalytic activity for CO oxidation. *Nano Res.* **2008**, *1*, 46–55.

[40] Ahmadi, T. S.; Logunov, S. L.; El-Sayed, M. A. Picosecond dynamics of colloidal gold nanoparticles. *J. Phys. Chem.* **1996**, *100*, 8053–8056.

[41] Zhang, J. Z. Ultrafast studies of electron dynamics in semiconductor and metal colloidal nanoparticles: Effects of size and surface. *Acc. Chem. Res.* **1997**, *30*, 423–429.

[42] Subramanian, V.; Wolf, E. E.; Kamat, P. V. Green emission to probe photoinduced charging events in ZnO–Au nano-particles. Charge distribution and Fermi-level equilibration. *J. Phys. Chem. B* **2003**, *107*, 7479–7485.

[43] Jakob, M.; Levanon, H.; Kamat, P. V. Charge distribution between UV-irradiated TiO$_2$ and gold nanoparticles: Determination of shift in the Fermi level. *Nano Lett.* **2003**, *3*, 353–358.